Microelectronic Engineering 209 (2019) 41–48

Contents lists available at ScienceDirect

Microelectronic Engineering

journal homepage: www.elsevier.com/locate/mee

Research paper

Process optimization of parameterized single shot method for a rapid production of photon sireve with direct write lithography

Kemal Rüzgar[a,b,*], Akin Bacıoğlu[a]

[a] Department of Physics Engineering, Hacettepe University, 06800 Beytepe, Ankara, Turkey
[b] TUBITAK Space Technologies Research Institute, 06800 Çankaya, Ankara, Turkey

ARTICLE INFO

Keywords:
Photon sieve
Direct write lithography
Microstructure fabrication
Diffractive optics
Parameterized single shot write

ABSTRACT

Photon sieves are promising elements for high-resolution optics. Fabrication of photon sieves is a raising topic of microscale optic fabrication. In order to fabricate photon sieves, many technics featured recently. Common production difficulties for fabrication are time consumption and complexity of process. This study provides direct write lithography process optimization for rapid and simple fabrication method. Using the direct write laser technology to pattern photoresist with parameterized single laser shot is the main idea of this study. Writing pattern with the parameterized single shot method gives good structures for photon sieves. Parameterized single shot method uses variable focus distance and modulation to write patterns with direct write lithography. Rapid patterning with better geometrical structures is the most important result of this study. In microscopic scale, geometrical results and time consumption are some drawbacks of continuous exposure laser method. It is inadequate for small structures such as photon sieves outermost pinholes. The main approach of this study is the optimization of the writing process for rapid and well-shaped production of smaller structures for photon sieves. The process optimization for Kloe direct write lithography system serves better structure for photon sieve pinhole than conventional writing methods.

1. Introduction

Photon sieve (PS) is a diffractive element, which consists of large number of pinholes with special distribution on Fresnel zones [1]. PS offers a promising solution for high-resolution imaging [1]. It has the potential to focus light to a very small spot, which is not limited by the width of the outermost zone as for the Fresnel zone plate (FZP) [2,3]. Diffractive optical elements are used for lithography systems [4] and especially as a diffractive optical element, photon sieves used for the fabrication of large space telescopes [5,6]. Several kinds of photon sieve models have been studied theoretically [7–9] and experimentally [10] to design different variety of photon sieves. Typically, photon sieves are fabricated by UV or electron beam lithography [11–13]. Also there are other methods for production photon sieves such as ion beam nanomachining [14] and x-ray lithography [15]. Lithographic process extend their usage with different areas, diffractive optical element machining is the one of the area of these. Production of photon sieves with laser system [16] and direct writing laser system is a novel development of this area [17,18]. Also there are some studies to simplify the production of diffractive optics [13,16,17]. In recent years, the rising of the costs for photomask has weakened the ability of mask based lithography to struggle with new methods [19,20]. The new techniques for lithographic process serve cost effectiveness and high resolutions for microscale fabrication. Some of these techniques are maskless optical-projection lithography (MOPL) [21,22] and zone-plate-array lithography (ZPAL) [4,23]. Maskless lithography serves cost effective production with some drawbacks. Time consumption for single sample is normal but on the other hand, single photomask can produce one more sample. Maskless lithography has to spend the same time for each sample. Recently some studies have been made to reduce the required time [16,17]. The newest techniques for the rapid production of micrometer scale structures is parameterized single shot method [24]. In this study, micrometer scale photon sieve structures are fabricated using negative tone photoresist. The effects of the fabrication parameters are investigated by using experimental techniques and rapid production technique also developed for photon sieve structures.

2. Method

In this section, we present our production system and theoretical bases that are used for experimental production. Our main method is photolithography with direct write laser system (DWLS). Our DWL

* Corresponding author at: Department of Physics Engineering, Hacettepe University, 06800 Beytepe, Ankara, Turkey.
E-mail address: kruzgar@hacettepe.edu.tr (K. Rüzgar).

https://doi.org/10.1016/j.mee.2019.03.014
Received 29 October 2018; Received in revised form 15 March 2019; Accepted 19 March 2019
Available online 20 March 2019
0167-9317/

system is Kloe Dilase 650. This system has one laser source with the wavelength of 375 nm and maximum output power is 84 mW. There are two optical line, which shape the beam for desired beam diameter (5 μm and 0.5 μm). Dilase 650 system has three main axes used to write pattern. These are one x-y stage to move the sample and z stage to move the objective for laser beam focusing. The system also has two different objective 10X and 40X (OLYMPUS UPLFLN 10X2, UPLFLN 40X) for focusing laser beam. The system has six main parameters used to write our pattern. These are stage speeds, optical path (beam diameter), focusing objectives, focusing distance, modulation and exposure times. In detail these parameters are modulation, relative energy from laser source. Speed, movement speed of stages (X-Y axes). Exposure time, laser source exposure time and focus distance is the distance from the best focus. In Ref. 21 the principles of maskless lithography is briefly explained. For fabrication the structure, we used negative tone photoresist, AZ nLof 2020 (Microchemicals, USA). For all fabrication, a 1.8 μm layer of AZ nLof 2020 photoresist was applied to glass (B270 test glass 25mmx1mm, clear) substrate. We have done our experiment with only writing on photoresist. There is no lift off or etching experiment have done in our experiments. For experimental production, we have seven conventional step for lithography. These are; cleaning substrate, spin coating of photoresist (Brewer Science Cee 200CBX spin coater was used), pre-bake, exposing, post-bake and development. All details of this process are given in Table 1.

To expose photoresist, we must obey the sufficient energy requirement. For AZ nLof 2020 photoresist, we nominally expose the resist with 66 mJ/cm^2 [25]. This parameter is important for rapid production method too. In this work, we have trials with variable exposure time, modulation, speed and focus distance. All of these parameters are related with minimum energy to expose the resist with suitable geometry.

There are three conventional and one rapid production method in this work. All of these works have done by direct write laser (DWL) system. All of direct laser production method, which discuss this paper, have same properties such as line width, optical path and objective (for concentric, spiral and linear method). For experimental production, also all lithographic steps kept constant. The Rapid production method, parameterized single shot method, processes the photoresist different way from the conventional three methods. Conventional methods use continuous laser beam and movement of stage. Three types of conventional writing methods are shown in Fig. 1a, b and c.

First method for producing circular geometry with filling is linear filling method. This method drawing geometry is shown in Fig. 1a. In this method, the system first draws a circular border, like all conventional methods, and later fills inside with horizontal or vertical lines. Horizontal or vertical lines can be drawn very fast with suitable modulation. Modulations for this system discovered in experimental study and showed in next section. Second method includes concentric circles for producing a circular filled shape. Border circular shape is filling with many concentric circles. Fig. 1b shows this filling geometry. Last conventional method of this study is the spiral fill method. In this method, there is spiral drawing to fill the inside of the circular border. Spiral filling has one time drawing capability and do not stop the laser during drawing.

Our rapid method is parameterized single shot method. This idea comes from circular shape of beam, which comes all optical paths. System focus laser beam on the photoresist with objective, which have circular aperture. Beam comes with variable cone angle with different focusing objective in this type DWL system. In this paper, we have calculated the dose and diameter of circular field to produce photon sieve pinhole. This method uses only single shot to produce circular geometry.

Table 1
Experimental production parameters of lithography.

Photoresist	AZ nLof 2020 (negative tone)
Spin Coating Parameters (Speed, Ramp, Time)	6000RPM 1000RPM 40s
Pre-Bake (Method, Time, Temperature)	Hot plate 120 s 110 °C
Exposure	Details is Given in Next Section
Post-Bake (Method, Time, Temperature)	Hot plate 60s 110 °C
Development (Developer, Time)	AZ 726 MIF 45 s

In conventional drawing and filling methods, we only use the speed and modulation of system. Other parameters are constant such as focus distance, at the best focus, and continuous laser exposing. In our new technique, we use single shot, which is parameterized with exposure time, speed of stage, modulation of laser and focus distance. In DWL system, we use OLYMPUS UPLFLN 40X (NA 0.75, see Fig. 3) objective to focus laser beam. The rapid production method has a variable focus distance for changing diameter of circular area of drawings. It is known that objectives have field of view like a cone shape. This gave us the idea for production of different diameter pattern with single shot. Changing focus distance changes the line width or simply beam radius on substrate. We use this property to obtain desired circular area. The most important parameter of this drawing is energy that exposes unit area. As the speed increase and keep the modulation same, the energy become insufficient to expose resist well. Therefore, the calculation of energy becomes important.

To calculate the modulation, we have to consider area of beam and energy per unit area. When all parameters except the modulation and focus distance are constant, only beam area changes. For this change, we have to change energy to obtain sufficient power to expose photoresist. Simple equation can give us how much energy we need to expose the resist well.

$$\frac{M_1}{r_1^2} = \frac{M_2}{r_2^2} \tag{1}$$

M_1 is the known modulation that exposes circular area with the radius r_1. r_2 is the radius of desired area and M_2 is the modulation required to supply for exposing the desired area sufficiently.

$$M_2 = M_1\frac{r_2^2}{r_1^2} \tag{2}$$

Cone angle gives the diameter of beam at given distance between substrate and objective. Numerical aperture is a property of objective and related with cone shape of beam. Distance between the substrate and objective plays significant role on beam diameter in variable focusing patterning (see;Fig. 2) [26].

To examine the experimental results, two imaging technique were used. First technique is optical microscopy, we used OLYMPUS BX53 optical microscope with objectives 5X, 10X, 20X, 50X and 100X (OLYMPUS UIS2 MPLANFLN 5X, 10X, 20X, 50X, 100x). The second imaging technique is optical profiling. ZYGO ZeGage™ Plus was used for profiling surface topography. Our optical profiler has three interferometric objective and the types of these objective are Mirau and Michelson. Objectives are 2.75X (Zygo Corp. NA 0.08, Michelson), 20X (Zygo Corp. NA 0.4 Mirau) and 50X (Zygo Corp. NA 0.55 Mirau).

3. Results and discussion

In this study, the first experimental result is speed-modulation effects of DWL system. This gives us the modulation and speed response of system.

Fig. 4 shows that slower speed and high modulation produce wider line. From theoretical basis, at same focus, the beam diameter is constant but more power on same point widen the diameter of processed spot. More power and speed makes change on spot radius with absorption and scattering effects. Conventional methods for writing patterns on photoresist have good results for straight line drawing. On the other hand, when pattern has circular drawings or turning points, writing speed must be decreased. Changing the speed on the drawing makes some difference on line widths. It can be seen from Fig. 4a and b.

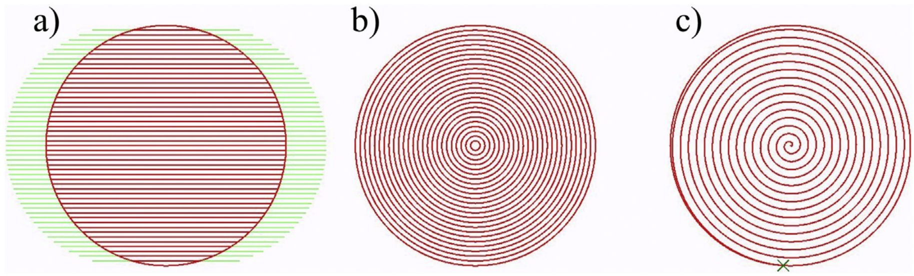

Fig. 1. Conventional direct write laser (DWL) drawing methods, a) line filling, b) concentric circular filling and c) spiral filling method.

When the laser draws the circular border, it must be slowed down to at least 0.25 mm/s to draw the border in circular geometry. Otherwise, it draws the geometry like a polygon. Fig. 5 shows the optical microscope image of the speed dependence of circular geometry.

Fast movement of stage causes the polygon geometry. Speed is not only problem for geometry; on the other hand, it is problem for time consumption. With the decreasing size of geometry, speed must be reduced too. To give information about the details of production and time, we also made experiments on the other conventional methods. Fig. 6a and b shows the profiler image of circular border with line filling method. Production time is different for this couple (see Fig. 6a and b).

Slower speeds give better border drawing but the time consumption is less preferable. In microscopic scale, we have already seen the non-circular region on border at slower speed. It can be beaten by much slower speeds. All conventional methods in this paper have the same problem in circular border drawings. In concentric circle method, there is no line and time consumption is different from the first method. Fig. 6c and d shows the optical profiler images of slower and faster speed drawings. With no straight line, geometry has better circularity. However, all circle drawings make this method slower than line fill geometry. The reason is the lines in linear fill method can be produced at a faster speed. The line filling method become slower with the speed of circular and spiral fill method. Its main reason is making discontinuous patterning with turning back to line start at every filling line. Third method is spiral fill method. Time requirement of this method is nearly same with circular fill method. Fig. 6e and f shows the difference between the slower and faster speed drawings of spiral fill method. All filling method in Fig. 6 keeps limit modulation to show pattern drawing clearly.

In this paper, we want to show much simpler and rapid production method for patterning small circular geometry. In all conventional method, we tightly bound the speed for good circular drawings. Unluckily when the structure is very small, the speed must be reduced too much. Even it was done, the structure may still be in polygon geometry. The last drawback that we calculated with system parameters is time consumption. Table 2 shows the writing durations of conventional methods.

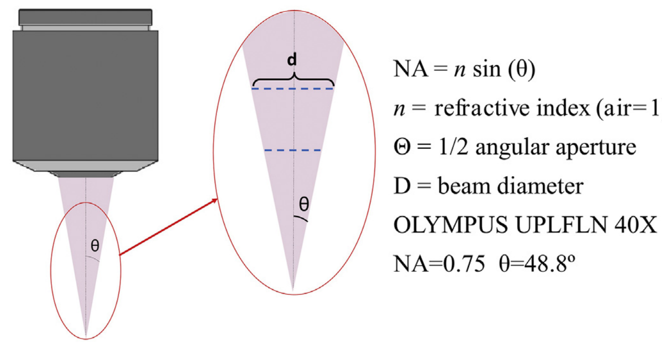

Fig. 3. Numerical aperture and cone angle for 40X, NA 0.75 objective.

Parameterized single shot method uses the advantage of focusing properties to change beam diameter. Fig. 7 shows the experimental results of focusing distance effect on line width.

With a single shot, we can obtain smaller structure than conventional methods. Fig. 8 shows the examples of single shot method. The variable parameters for single shot method are exposure time, speed, modulation and focus distance.

Detailed experiments on single shot parameters are tried. First parameter that affects the single shot drawing is speed. Speed directly affects the circular structure. Like the conventional method, speed makes great difference on geometry of circularity. Nevertheless, it is different from conventional methods. Fig. 9 shows the speed dependence of circular geometry of drawing.

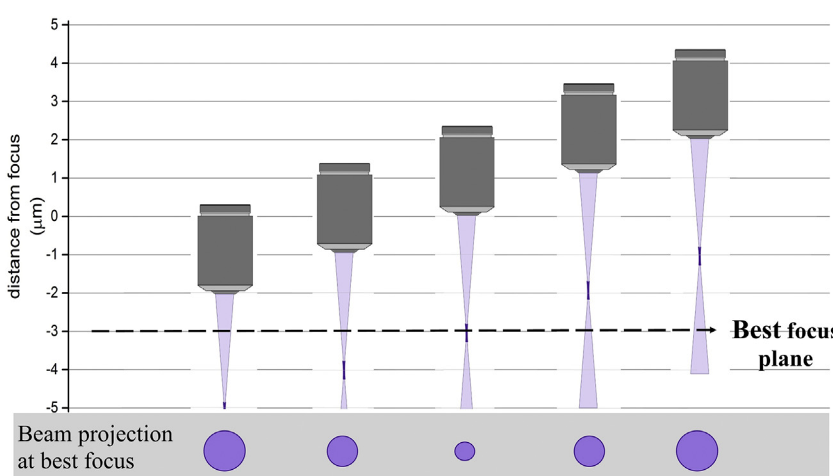

Fig. 2. Schematic view of beam diameter related with objective focus distance.

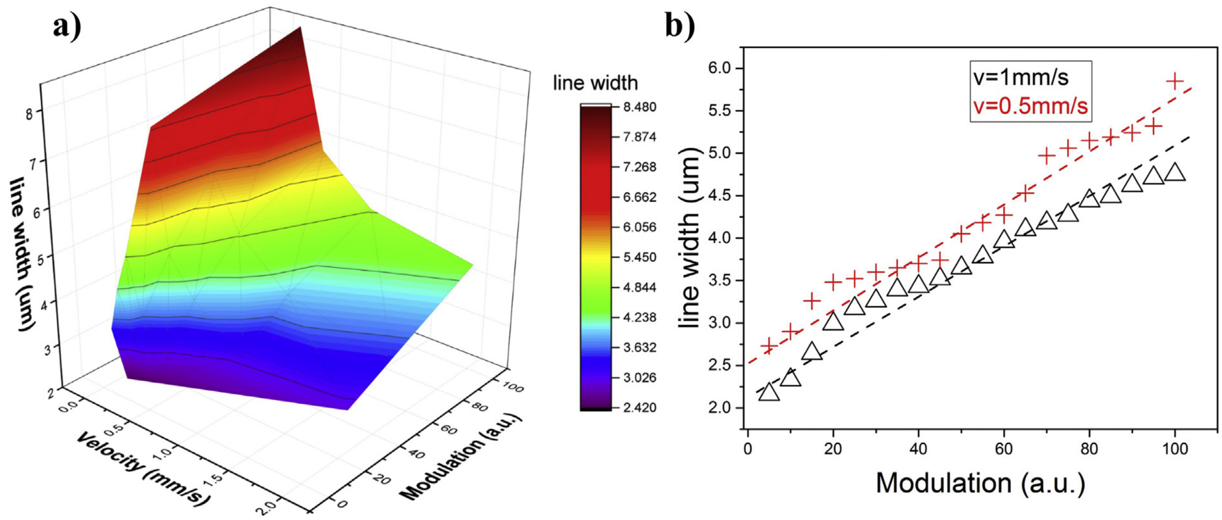

Fig. 4. Modulation – speed relation of line drawing. a) 3D graph of different speed and modulation data b) 2D graph of v = 0.5 and v = 1 mm/s lines. (All other system parameters are constant).

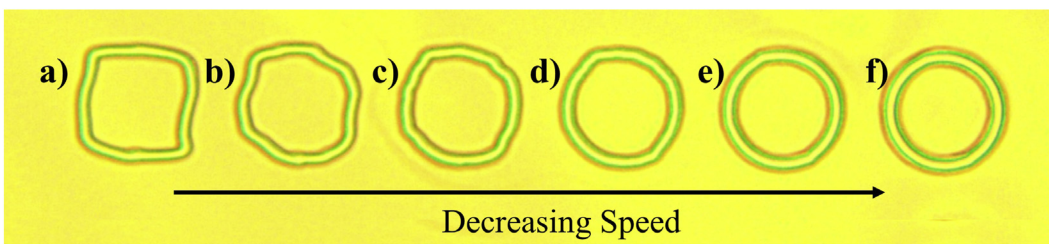

Fig. 5. Optical microscope image of different speed circular drawings. a) 1.5, b) 1, c) 0.5, d) 0.25, e) 0.1 and f) 0.05 mm/s.

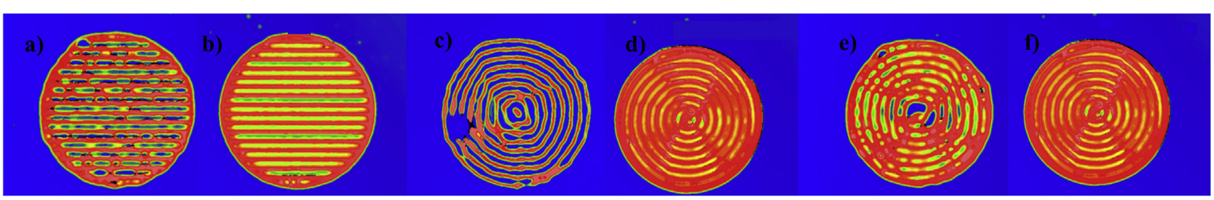

Fig. 6. Profiler images of filling method. Velocities are a) v = 0.5 mm/s b) v = 0.1 mm/s for linear fill method, c) v = 0.5 mm/s d) v = 0.1 mm/s for circular fill method and e) v = 0.5 mm/s f) v = 0.1 mm/s for spiral fill method.

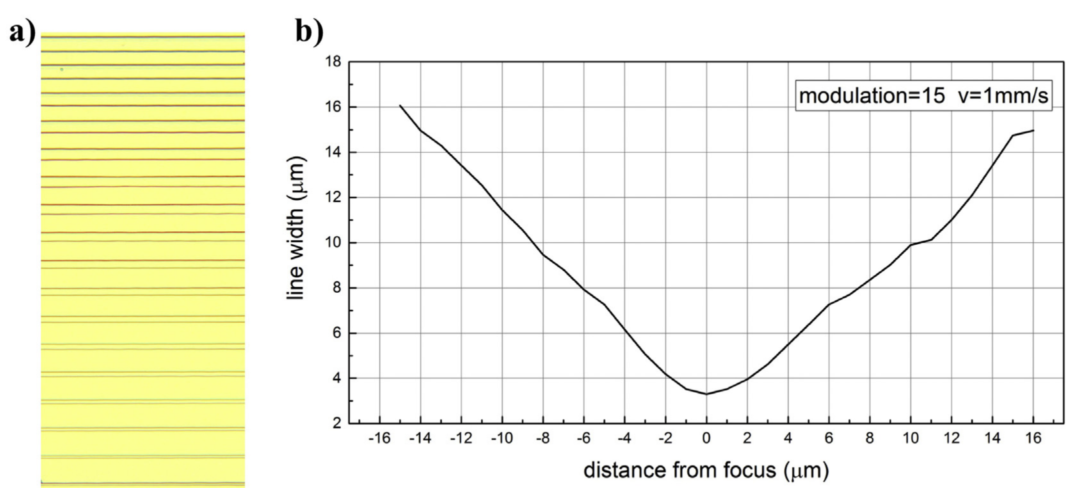

Fig. 7. a) Optical microscope image of lines with different focus distance and b) numerical results of focusing distance effects on line width.

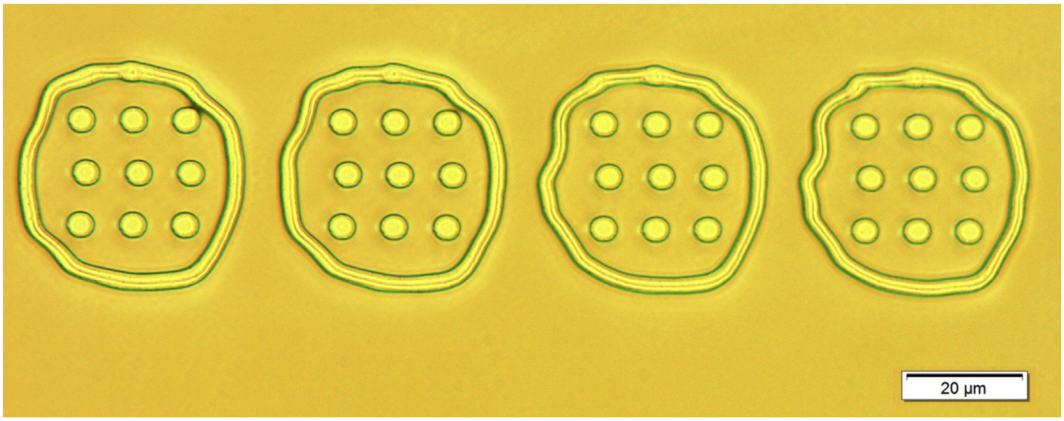

Fig. 8. Single shot laser points on photoresist (outer ring were drawn with speed of 1 mm/s).

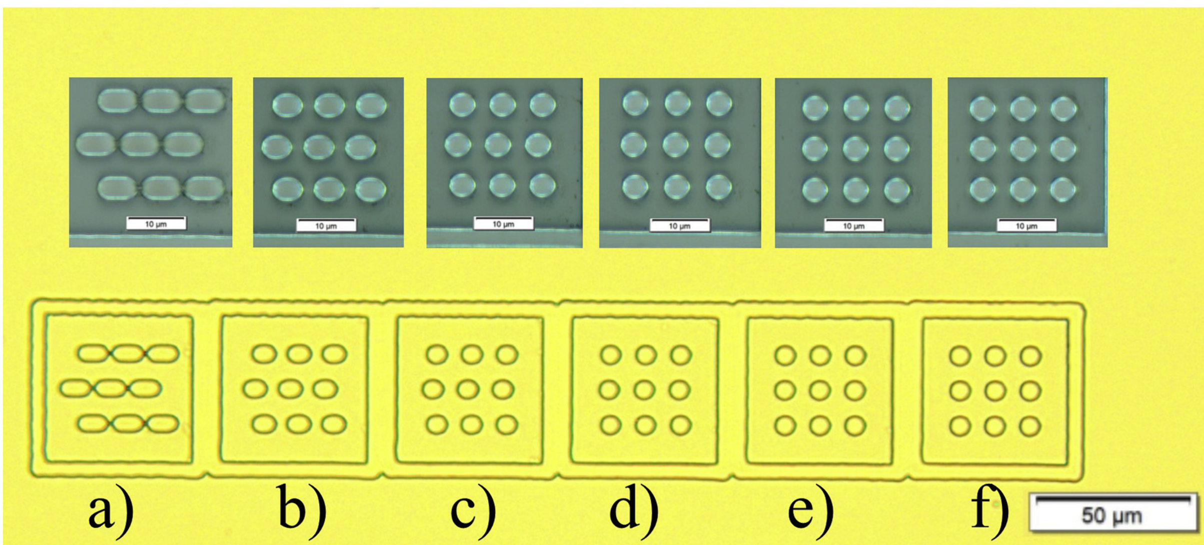

Fig. 9. Optical microscope image of single shot laser at different velocities. Velocities are a) 0.1, b) 0.05, c) 0.025, d) 0.01, e) 0.005 and f) 0.0025 mm/s (modulation 100 and exposure time 0.05 s, bottom figures have smaller magnifying value and tops are bigger).

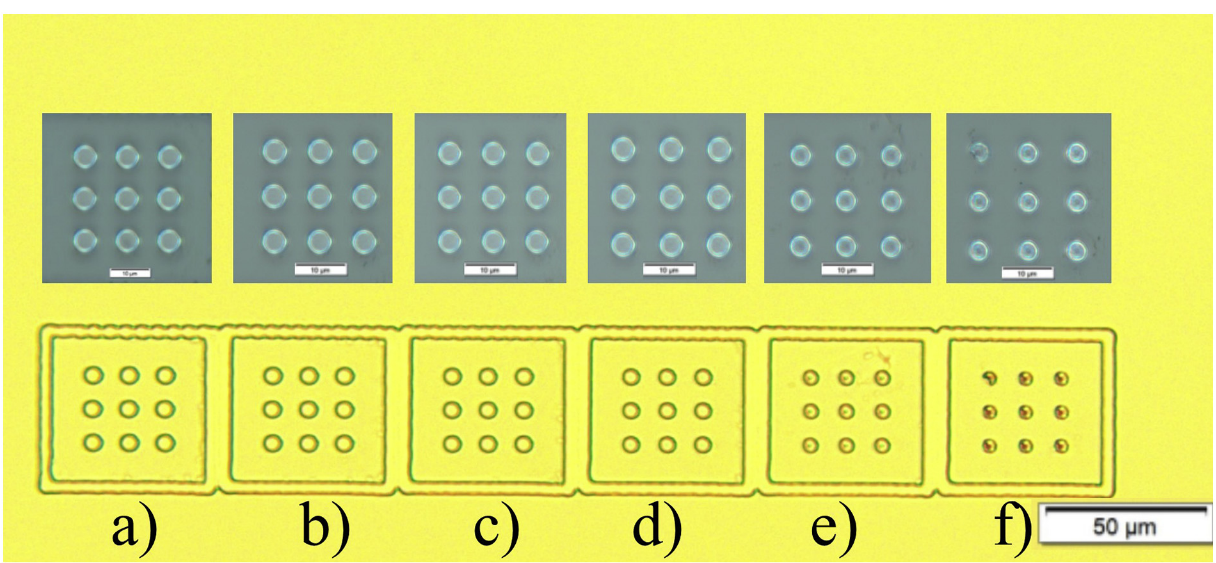

Fig. 10. Optical microscope image of single shot laser with different exposure times. Exposure times a) 0.05, b) 0.04, c) 0.03, d) 0.04, e) 0.01 and f) 0.005 s (modulation 40 and speed 0.005 mm/s, bottom.

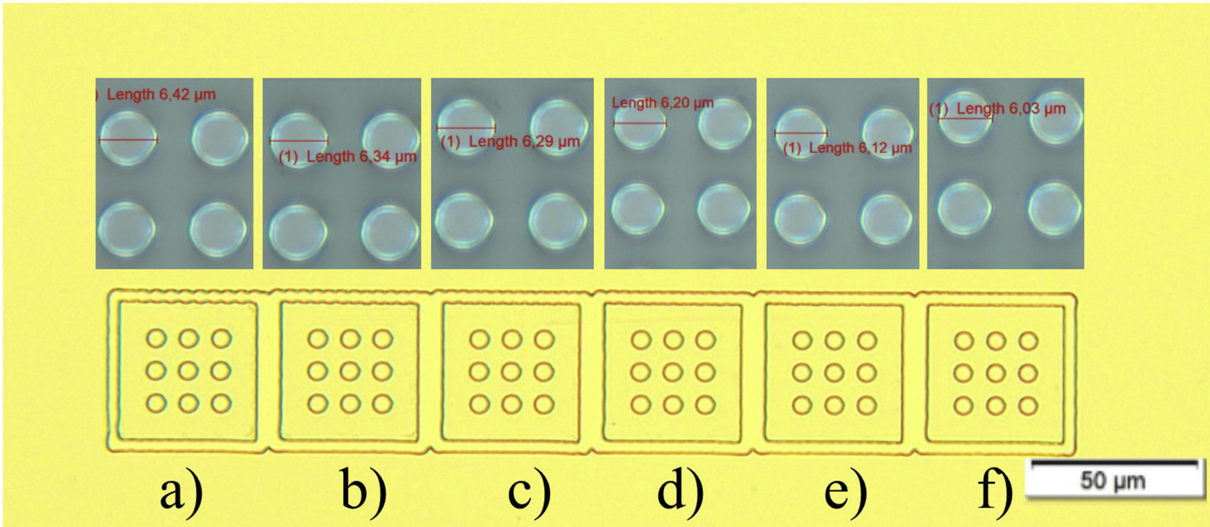

Fig. 11. Optical microscope image of single shot laser with different modulations. Modulations are a) 100, b) 90, c) 80, d) 70, e) 60 and f) 50 (speed 0.005 mm/s, exposure time 0.005 s, bottom figures have smaller magnifying value and tops are bigger).

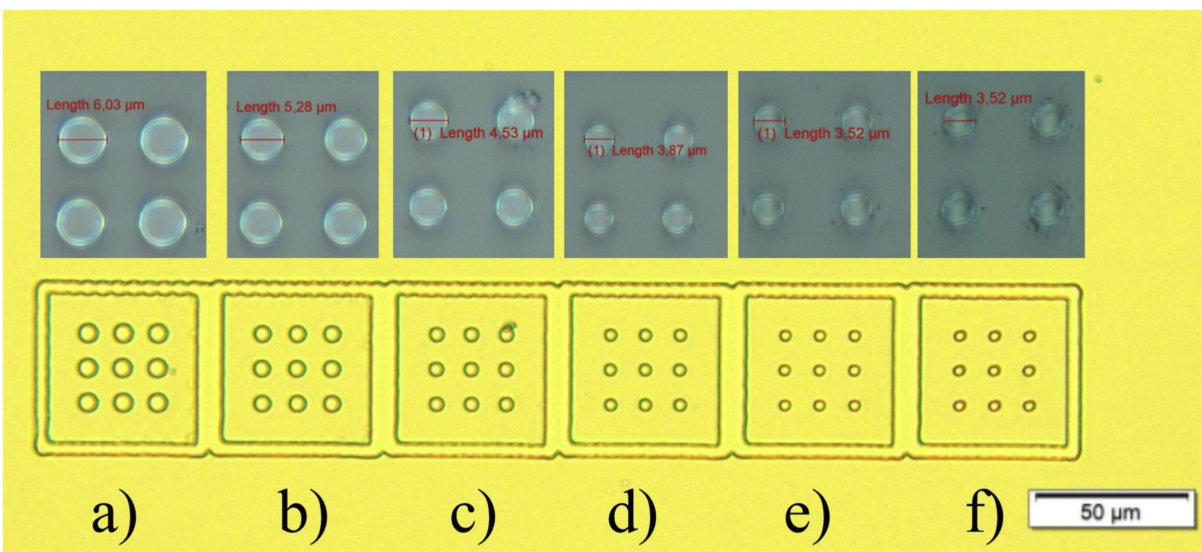

Fig. 12. Optical microscope image of single shot laser with different focus distance. Distance from the best focus a) +5 µm, b) +4 µm, c) +3 µm, d) +2 µm, e) +1 µm, and f) at the best focus (speed 0.005 mm/s, exposure time 0.005 s Modulation 100, bottom figures have smaller magnifying value and tops are bigger).

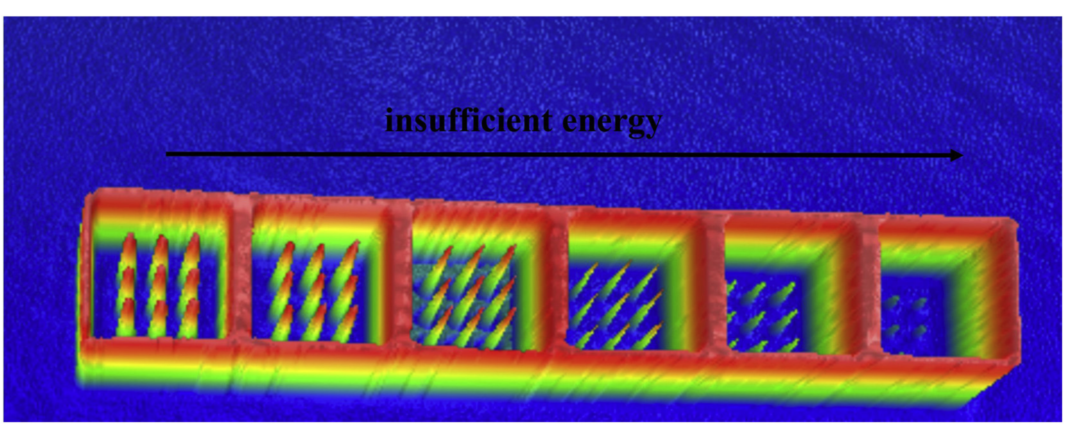

Fig. 13. Optical profiler image of insufficient energy distribution for different structure diameter.

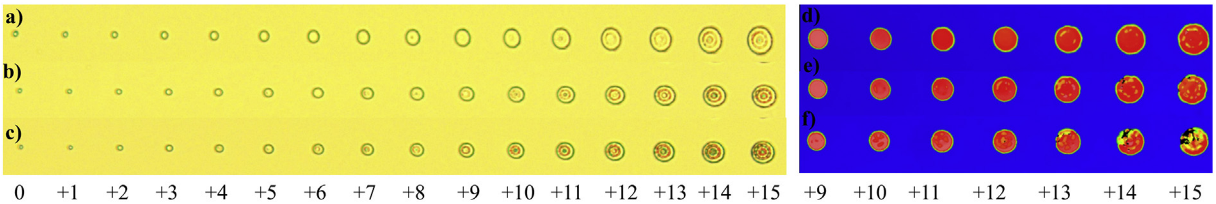

Fig. 14. Optical microscope image of velocity 0.005 mm/s, modulation 25–100 and focus 0-15 μm trials with exposure time a) 0.005 s b) 0.01 s c) 0.015 s. Optical profiler image of modulation 70–100 and focus 9–15 with exposure times e) 0.005 s d) 0.01 s f) 0.015 s.

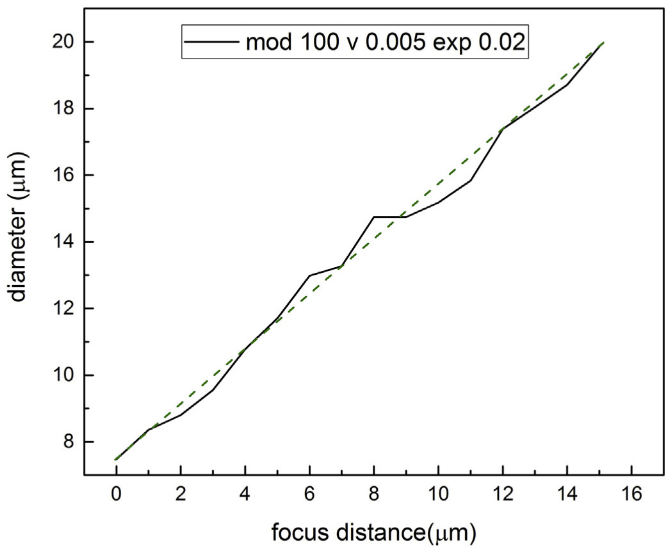

Fig. 15. Focus distance dependence of structure diameter (modulation 100, speed 0.005 mm/s and exposure time 0.02 s, dot lines gives linear behavior of variation).

Faster speed gives elliptical geometry. It comes from the relation between speed of stages and exposure time. We simply obtain the result (see Fig. 9a) with high exposure time and high speed of stages. It affects the geometry adversely. It can be easily overcome with suitable exposure time and modulation for faster speed. Unlikely conventional methods speed hardly effect the beam diameter. On the other hand, it mostly affects the pattern shape. The second important parameter is exposure time. Exposure time changes the circular geometry as well as diameter of structure, but not so much like speed. Fig. 10 shows the exposure time dependence. In trials, showing in Fig. 10, we kept all of the other parameters constant except exposure time.

For exposure time trials, the speed is low enough to keep circular geometry for several exposure times. When exposure time increases and speed is high enough, the geometry gets out of order and takes the elliptical shape as shown Fig. 9a. On the other hand, when exposure time decrease, insufficient energy absorbed by photoresist, which is seen at Fig. 10f. It must be kept at optimum value for better patterning.

Other important parameters for fabrication are modulation and focus distance. The modulation difference changes the diameter of structures. Fig. 11 shows the different modulation at constant speed and

Table 2
100 μm diameter hole filling times with conventional methods (other all parameters of system are constant).

Speed (mm/s)	Linear filling time (s)	Concentric circular filling time (s)	Spiral filling time (s)
0.1	94	28	30
0.01	931	277	292

Table 3
Modulation and focus dependence of structure diameter (note: The best focus gives the smallest diameter).

Focal distance (μm)	Modulation (rel.)	Structure diameter (μm)
+5	50	6.42
+5	60	6.34
+5	70	6.29
+5	80	6.20
+5	90	6.12
+5	100	6.03
+0	100	3.52
+1	100	3.52
+2	100	3.87
+3	100	4.53
+4	100	5.28
+5	100	6.03

exposure times. The biggest modulation has the biggest diameter of structure like the line width, which was discussed before. Table 3 gives modulations and beam diameters.

The most important parameter taken into account is focus distance for this method. In method section, the focusing properties and beam diameter calculation technique was given. The right production method with focus difference is related with the energy absorbed per unit area to expose photoresist well. Fig. 12 shows the focus distance and beam diameter relation for single shot.

Table 3 gives the diameter of structure at 0 μm and + 1 μm is same. This value comes from the focal depth of objective. For the 40X objective this value is normal. When smaller NA objective is used, the focal depth comes bigger and the focus distance affects the structure diameter lesser [27].

The last important parameter that we tried in this work is the dose of energy to expose photoresist. If the energy is not enough to expose the resist well, lithography parameter, especially lift-off mechanism falls in danger. Because of this reason, optical microscope is insufficient

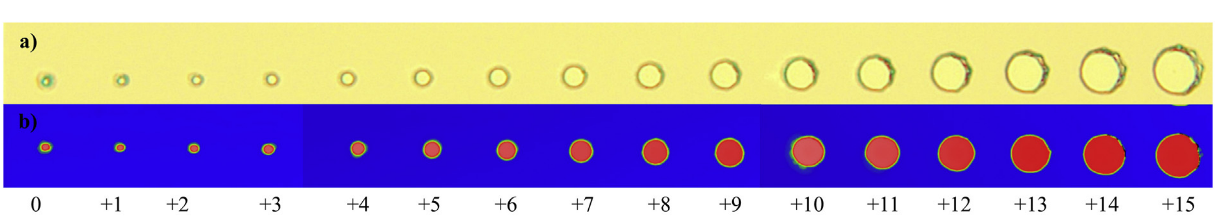

Fig. 16. a) Optical microscope image b) optical profiler image of focus difference (0-15 μm) and structure diameter relation.

Table 4
Calculated modulation for different focus distance and related diameter.

Focal distance (μm)	Diameter (μm)	Modulation	Focal distance (μm)	Diameter (μm)	Modulation
0	4.18	5.65	+8	11.44	42.34
+1	4.84	7.58	+9	12.34	49.27
+2	5.5	9.79	+10	12.98	54.51
+3	5.96	11.50	+11	13.64	60.20
+4	7.04	16.04	+12	14.52	68.22
+5	8.36	22.61	+13	15.62	78.94
+6	8.81	25.11	+14	16.51	88.20
+7	10.34	34.59	+15	17.58	100

to investigate this property of processed resist. We used optical profiler, instead, to see the topography of structure. Fig. 13 shows the example of insufficient energy to expose the resist well.

To investigate the absorbed energy, related with beam diameter, we made experiments with different focus but the same energy values. Fig. 14 shows the experimental results of these investigations. The experiment of modulation-focus dependence has three different modulations group and expose time. All experiments on this trial have same modulation at same focus distance. It starts from the best focus and modulation 25 and goes on with increasing parameters. Increasing parameters are 1 μm step in focus distance and 5 (relative) step in modulation. The final focus distance is 15 μm and modulation 100. These trials give us the best energy value for the largest focus distance. Other parameters, the speed of the beam and exposure time is constant.

Experiments on different parameters also give us the relation between the focus distance and diameter of structures. As shown in method section the modulation variation can be calculated with simple formula to expose the photoresist with sufficient energy. Diameter variation is revealed by experiments. Fig. 15 shows the relation between focus distance and structure diameter for specific exposure time, modulation and speed.

Table 4 also shows the modulation value related with diameter.

Calculated modulations applied to the same pattern that was written in Fig. 14. Fig. 16 shows new results.

Calculated modulation gives good performance to expose film at different focus. It must be noted that the modulation parameter is very important for maintaining of the lithography process.

4. Conclusion

We have demonstrated parameterized single shot method for the rapid production of microscale photon sieve structures. Photon sieve pinhole was pattern on photoresist and successfully verified the advantage of rapid production for circular geometry. The influence of several parameters on the production of pinholes, such as focusing distance and modulation has been evaluated by experimental results. Another remarkable improvement is the production of small pinholes by direct laser method, which is hardly produced by conventional methods. Maskless lithography has the disadvantages of time consumption against to conventional lithography. It must draw the whole patterns again for each sample. Based on the work presented here, we conclude that rapid production of pinholes reduces the maskless lithography time problem. From the experiments, we have showed, line width of patterns are useless below few micrometer sized pinholes. On the other hand, the parameterized single shot method gives better result with smaller circular structure.

In summary, we have demonstrated a technique for the rapid production of pinholes and the experimental details. This technique is also useful for the other microscale circular geometry. In addition, parameterized single shot method promises the improvement on maskless lithography process such as dot matrix lithography.

Acknowledgments

The author would like to thank Adem Yenisoy for helpful suggestions. This work was supported by TUBITAK Space Technologies Research Institute OPMER project (project no. 7P160700).

References

[1] L. Kipp, et al., Sharper images by focusing soft X-rays with photon sieves, Nature 414 (6860) (2002) 184–188.
[2] C. Hou, Novel diffractive optical element: binary photon sieve, Opt. Eng. 50 (6) (2011) (068001).
[3] I. Minin, O. Minin, FDTD analysis of millimeter wave binary photon sieve Fresnel zone plate, Open J. Antennas Propag. 01 (03) (2013) 44–48.
[4] D. Gil, R. Menon, H.I. Smith, The promise of diffractive optics in maskless lithography, Microelectron. Eng. 73-74 (2004) 35–41.
[5] G. Andersen, Large optical photon sieve, Opt. Lett. 30 (22) (2005) 2976.
[6] G. Andersen, Membrane photon sieve telescopes, Appl. Opt. 49 (33) (2010) 6391.
[7] Q. Cao, J. Jahns, Focusing analysis of the pinhole photon sieve: individual far-field model, J. Opt. Soc. Am. A Opt. Image Sci. Vis. 19 (12) (2007) 2387.
[8] Q. Cao, J. Jahns, Nonparaxial model for the focusing of high-numerical-aperture photon sieves, J. Opt. Soc. Am. A 20 (6) (2007) 1005.
[9] Z.L. Zhang, Q. Cao, X. Lu, Focusing contribution of individual pinholes of a photon sieve: dependence on the order of local ring of underlying traditional Fresnel zone plate, Chin. Opt. Lett. 8 (3) (2010) 256–258.
[10] C. Zhou, X. Dong, L. Shi, C. Wang, C. Du, Experimental study of a multiwavelength photon sieve designed by random-area-divided approach, Appl. Opt. 48 (8) (2009) 1619.
[11] R. Menon, D. Gil, G. Barbastathis, H.I. Smith, Photon-sieve lithography, J. Opt. Soc. Am. A 22 (2) (2005) 342.
[12] N.W. Parker, A.D. Brodie, J.H. McCoy, A high throughput NGL electron beam direct-write lithography system, Proc. SPIE 3997 (2000).
[13] D. Gil, R. Menon, H.I. Smith, Fabrication of high-numerical-aperture phase zone plates with a single lithography exposure and no etching, J. Vac. Sci. Technol. B Microelectron. Nanom. Struct. 21 (6) (2003) 2956.
[14] R. Janeiro, R. Flores, P. Dahal, J. Viegas, Fabrication of a phase photon sieve on an optical fiber tip by focused ion beam nanomachining for improved fiber to silicon photonics waveguide light coupling, Opt. Express 24 (11) (2016) 11611.
[15] W. Jiang, et al., Fabrication of submicron photon sieve using E-beam lithography and X-ray lithography, Microelectron. Eng. 88 (10) (2011) 3178–3181.
[16] M.N. Julian, D.G. MacDonnell, M.C. Gupta, Fabrication of photon sieves by laser ablation and optical properties, Opt. Express 25 (25) (2017) 31528.
[17] M.P. Lim, X. Guo, E.L. Grunblatt, G.M. Clifton, A.N. Gonzalez, C.N. Lafratta, Augmenting mask-based lithography with direct laser writing to increase resolution and speed, Opt. Express 26 (6) (2018) 7085.
[18] N. Tsutsumi, et al., Direct laser writing for micro-optical devices using a negative photoresist, Sci. Opt. Mater. Express Opt. Express 25 (25) (2017) 31539.
[19] D.J. Resnick, et al., Imprint lithography for integrated circuit fabrication, J. Vac. Sci. Technol. B Microelectron. Nanom. Struct. 21 (6) (2003) 2624.
[20] D. Elfström, et al., Mask-less ultraviolet photolithography based on CMOS-driven micro-pixel light emitting diodes, IEEE Photon. Technol. Lett. Lab Chip OSA J. Vac. Sci. Technol. B J. Vac. Sci. Technol. B 17 (26) (2009) 23522.
[21] OML: optical maskless lithography for economic design prototyping and small-volume production.
[22] N. Choksi, et al., Maskless extreme ultraviolet lithography, J. Vac. Sci. Technol. B Microelectron. Nanom. Struct. 17 (6) (2002) 3047.
[23] R.F. Pease, Maskless lithography, Microelectron. Eng. 78-79 (1-4) (2005) 381–392.
[24] N.J. Jenness, R.T. Hill, A. Hucknall, A. Chilkoti, R.L. Clark, A versatile diffractive maskless lithography for single-shot and serial microfabrication, Opt. Express 18 (11) (2010) 11754.
[25] AZ ® nLOF™, Series, www.microchemicals.com/micro/tds_az_nlof2000_series.pdf, (2000).
[26] M.W. Davidson, https://www.microscopyu.com/tutorials/nuaperture.
[27] T. Ito, S. Okazaki, Pushing the limits of lithography, Nature. 406 (2000) 1027–1031.